

A Novel Comprehensive Multiport Network Model for Stacked Intelligent Metasurfaces (SIM) Characterization and Optimization

Andrea Abrardo, *Senior Member, IEEE*, Giulio Bartoli *Member, IEEE*, Alberto Toccafondi, *Senior Member, IEEE*

Abstract—Reconfigurable Intelligent Surfaces (RIS) are transformative technologies for next-generation wireless communication, offering advanced control over electromagnetic wave propagation. While RIS have been extensively studied, Stacked Intelligent Metasurfaces (SIM), which extend the RIS concept to multi-layered systems, present significant modeling and optimization challenges. This work addresses these challenges by introducing a new optimization framework for heterogeneous SIM architectures that, compared to previous approaches, is based on a comprehensive model without relying on specific assumptions, allowing for a broader applicability of the results. To this end, we first present a model based on multi-port network theory for characterizing a general electromagnetic collaborative object (ECO) and derive a general framework for ECO optimization. We then introduce the SIM as an ECO with a specific architecture and provide insights into SIM optimization for various architectures, discussing the complexity in each case. Next, we analyze the impact of commonly used assumptions, and as a further contribution, we propose a backpropagation algorithm for implementing the gradient descent method for a simplified SIM configuration.

I. INTRODUCTION

Reconfigurable Intelligent Surfaces (RIS) represent an innovative technology for next-generation wireless networks, particularly in the context of mmWave frequencies [1]–[3]. Most optimization works model RIS as planar arrays of reflective elements whose impedances can be adjusted to create controllable phase-shifts, shaping the reflected wavefront. However, these models often lack electromagnetic consistency, not fully accounting for factors critical to realistic RIS operation [4], [5]. Recent advancements highlight the necessity of accurate reradiation models, combining surface-level optimization with precise design of RIS elements [6]. Multiport network theory has emerged as an effective method for ensuring the accuracy of models while enabling easy system-level optimization [7]–[12]. New approaches based on S and Z parameters reveal the limitations of classical RIS models that treat them as ideal scatterers, often neglecting important aspects such as electromagnetic mutual coupling, the presence of unwanted reflections, and the correlation between reflection coefficient phase and amplitude [13], [14]. Incorporating these factors leads to more robust end-to-end models capable of optimizing all scattering components and minimizing unwanted interferences.

The authors are with the University of Siena and CNIT. Email: abrardo@unisi.it, giulio.bartoli@unisi.it, alberto.toccafondi@unisi.it.

Initial research on RIS primarily focused on single-connected, reflective RIS models, characterized by diagonal phase-shift matrices. However, the limitations of these simplified models—particularly in terms of flexibility and scalability—have motivated the development of more advanced metasurface-based systems. Among these, particular emphasis is placed on the so-called beyond-diagonal structures, in which different ports of the RIS are interconnected through programmable lines, creating more complex and flexible structures [15]. In this context, in addition to traditional purely reflective RIS, hybrid transmissive and reflective structures have also been considered, which are referred to as simultaneously transmitting and reflecting RIS (STAR-RIS) [16]. Just as with classical RIS, in these more complex architectural scenarios, the traditional approach to managing the complexity of optimization typically involves relying on certain assumptions, which can limit the generality of the results.

Recently, a novel technology relying on stacked intelligent metasurfaces (SIM) has emerged by cascading multiple RIS [17], which is capable of implementing signal processing in the EM wave regime. This represents a significant advancement, providing improved control over wave propagation and greatly increasing the degrees of freedom [18]. In a SIM, each intelligent metasurface acts like a layer in a Deep Neural Network (DNN), while each programmable meta-atom functions similarly to a neuron, possessing adjustable phase and amplitude responses that can be tailored to meet various task needs and adapt to changing environments. Consequently, SIM benefits from the strong representation capabilities of Artificial Neural Networks (ANNs), the exceptional speed of electromagnetic (EM) computing, and the energy-efficient tuning properties of metasurfaces.

Although the literature on SIM is still limited, it is rapidly expanding due to the significant interest in this topic. SIMs have been shown to effectively perform beamforming in the electromagnetic domain and to implement holographic multiple-input multiple-output communications without requiring excessive radio-frequency (RF) chains [18], [19]. Moreover, SIM can be used to enhance the performance of multi-user beamforming [20]–[22]. In [23] the achievable rate of a large SIM-aided system with statistical CSI is derived and an optimization procedure based on AO is proposed. In [24] a deep reinforcement learning approach is proposed to overcome limitations

of traditional AO approaches. The use of SIM in cell-free networks is explored in [25] for the downlink and in [26] for the uplink, where the multi-user beamforming is designed for a system where each AP has its own SIM. Moreover, the work in [27] considers a LEO satellite equipped with a SIM. Some works focus on near field communications, such as [28] where users are equipped with multiple antennas, and [29], where the diffraction behavior of SIM meta-atoms is taken into account. Furthermore, SIMs can be used to improve sensing performance, as for example the estimation of direction of arrival can be enhanced by the use of the SIM, as analyzed in [30] and [31], and the use of SIM for ISAC problems has been studied in [32]–[34].

Despite the promise of SIM, accurate and tractable modeling remains a significant challenge. Existing research employs a simple model in which the SIM is characterized as a cascade, consisting of the propagation through the channels that separate the layers, along with the phase shifts introduced during the transition through each layer. An important effort to provide a more accurate model, highlighting the intrinsic approximations in the simplified model previously used for SIM optimization, is presented in [35]. However, even in this work, the analysis of SIM performance relies on the usual assumptions that enable the use of the simple cascade model, specifically by assuming ideal RISs without mutual coupling and employing a unilateral approximation for propagation through the channels separating the layers of the constituent RISs in the SIM. This last approximation requires the presence of non-reciprocal propagation environments, making the realization of such a SIM a challenging problem. It remains an open question whether SIM can deliver the promising performance suggested by initial studies, even in cases where the commonly considered approximations may not hold true.

II. CONTRIBUTIONS

This work aims to provide a comprehensive analysis of SIM systems. The main contributions are:

- 1) **General ECO Model:** A thorough multiport network model of a general electromagnetic collaborative object (ECO) is introduced, generalizing previous models for diagonal RIS, non-diagonal RIS, STAR-RIS, and SIM. Then, an optimization procedure based on gradient descent is developed without relying on specific assumptions or approximations.
- 2) **Complete SIM Model:** The general ECO model is specialized for the SIM case. Hence, the gradient-descent-based optimization approach is tailored to the SIM case, highlighting the complexity reduction afforded by the SIM architecture compared to the general ECO case.
- 3) **Simplified SIM Models and Backpropagation Algorithm:** Several simplifications of the general SIM model are analyzed, focusing on SIM based on diagonal RIS and the unilateral approximation. For the case most frequently considered in the literature (ideal diagonal RIS and unilateral approximation), a backpropagation algorithm

is proposed to significantly reduce computational complexity. The limitations of these common approximations are discussed in the context of practical implementation challenges.

III. GENERAL MULTI-PORT MODEL

Let's consider the multiport system model shown in Fig. 1, which is a general framework for characterizing a transmitter with L ports (e.g., a multi-antenna transmitter), a receiver with M ports (e.g., a multi-antenna receiver), along with N ports corresponding to N elements of an object that receives, processes, and retransmits electromagnetic waves to and from the wireless channel. This object can generically represent a RIS, whether reflective or transmitting or operating in both modes, such as a Simultaneously Transmitting And Reflecting RIS (STAR-RIS), or a Stacket Intelligent Metasurfaces (SIM). To remain general, let's call this object an ElectroMagnetic Collaborative Object (ECO). The Z-parameters representation of the multiport network relates the voltages V and the currents I at the ports as follows:

$$\begin{bmatrix} \mathbf{V}_T \\ \mathbf{V}_E \\ \mathbf{V}_R \end{bmatrix} = \begin{bmatrix} \mathbf{Z}_{TT} & \mathbf{Z}_{TE} & \mathbf{Z}_{TR} \\ \mathbf{Z}_{ET} & \mathbf{Z}_{EE} & \mathbf{Z}_{ER} \\ \mathbf{Z}_{RT} & \mathbf{Z}_{RE} & \mathbf{Z}_{RR} \end{bmatrix} \begin{bmatrix} \mathbf{I}_T \\ \mathbf{I}_E \\ \mathbf{I}_R \end{bmatrix},$$

where \mathbf{I}_x and \mathbf{V}_x for $x \in \{T, E, R\}$ denote the currents and voltages at the ports of the transmitter (T), ECO (E), and receiver (R). Moreover, the voltages and the currents at the ECO ports are related as $\mathbf{V}_E = -\mathbf{Z}_E \mathbf{I}_E$, where \mathbf{Z}_E is the impedance matrix of the network to which the RIS ports are connected.

The presented model is a generic multi-port network model that has been studied in the literature, primarily in the context of RIS, for which the transfer function $\mathbf{H}_Z = \frac{\mathbf{V}_R}{\mathbf{V}_T}$ is known. In particular, as shown in [13], in the case of maximum power transfer, meaning that all transmitter and receiver ports are match-terminated at Z_0 , we have:

$$\mathbf{H}_Z = \frac{1}{4Z_0} [\mathbf{Z}_{RT} - \mathbf{Z}_{RE}(\mathbf{Z}_{EE} + \mathbf{Z}_E)^{-1}\mathbf{Z}_{ET}]. \quad (1)$$

This model therefore generally represents the relationship between the output and input signals in a system containing an ECO. Note that, in the case the ECO is a RIS, if the network to which the RIS elements are connected is such that each RIS element is terminated in its own impedance and is not connected to others, we have a classical diagonal RIS. On the other hand, if the network also includes connections between different RIS elements, we have a non-diagonal RIS also called beyond-diagonal RIS (BD-RIS) [15]. Furthermore, if the load network allows some RIS elements to let the signal pass through to other RIS elements, the same model can describe a RIS operating in transmissive mode, where some elements receive the signal and others transmit it [16]. Finally, if we divide the ECO ports into electromagnetically isolated groups comprising some receiving ports and some transmitting ports, we can also describe a SIM in which each group is a couple of tx/rx RISs

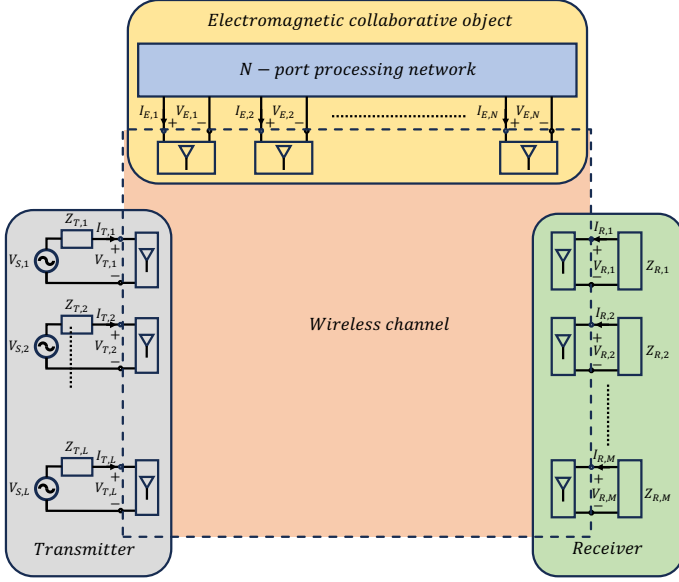


Fig. 1: Network model.

representing a layer of the SIM. The model is thus general, and to use it in optimizing the operation of the ECO it is necessary to adequately handle the nonlinear part of the transfer function, which includes the matrix inversion and depends on the controllable or tunable parameters of the ECO, i.e., the load network \mathbf{Z}_E .

IV. PROCESSING IN THE ELECTROMAGNETIC DOMAIN

Let us assume that the load network depends on a certain number P of controllable parameters and let us denote $\boldsymbol{\eta} \in \mathbb{C}^{P \times 1}$ the vector of controllable parameters, with the resulting \mathbf{Z}_E expressed as $\mathbf{Z}_E(\boldsymbol{\eta})$. To remain general, let then $\mathbf{A} \in \mathbb{C}^{M \times N}$ be a matrix which may include the receiver-ECO impedance matrix \mathbf{Z}_{RE} , as well as a linear filter used to extract an estimate of the transmitted signal. It can also be utilized to implement generic processing of the signal received by the ECO by, for example, using M probes to detect the received signal. Additionally, let $\mathbf{b} \in \mathbb{C}^{N \times 1}$ be the vector received at the ECO. Moreover, define $\mathbf{T}(\boldsymbol{\eta}) = (\mathbf{Z}_{EE} + \mathbf{Z}_E(\boldsymbol{\eta}))^{-1}$ and consider:

$$\mathbf{h}_T(\boldsymbol{\eta}) = \mathbf{A}\mathbf{T}(\boldsymbol{\eta})\mathbf{b}, \quad (2)$$

The transfer function defined in (2) represents a generic transfer function that includes the effect of the ECO and can be used to optimize the ECO in various application scenarios. Below, we present a general ECO optimization problem that can be adapted to different contexts of electromagnetic processing. Specifically, we consider the problem of designing the ECO such that, given an input \mathbf{b} , it produces an output that 'closely approximates' an output $\mathbf{x} \in \mathbb{C}^{M \times 1}$. To achieve this, we first introduce $\mathbf{h}_T = \mathbf{A}\mathbf{T}(\boldsymbol{\eta})\mathbf{b}$ and denote the squared error as $\epsilon(\boldsymbol{\eta})$:

$$\epsilon(\boldsymbol{\eta}) = (\mathbf{h}_T(\boldsymbol{\eta}) - \mathbf{x})^H (\mathbf{h}_T(\boldsymbol{\eta}) - \mathbf{x}). \quad (3)$$

Elaborating from (3), we get:

$$\epsilon(\boldsymbol{\eta}) = \mathbf{h}_T^H(\boldsymbol{\eta})\mathbf{h}_T(\boldsymbol{\eta}) - 2\Re(\mathbf{x}^H\mathbf{h}_T(\boldsymbol{\eta})) + \mathbf{x}^H\mathbf{x} \quad (4)$$

We then consider the following problem:

$$\min_{\boldsymbol{\eta}} \epsilon(\boldsymbol{\eta}). \quad (5)$$

To find an efficient strategy for solving the problem (5), it is necessary to calculate the gradient $\nabla_{\boldsymbol{\eta}}\epsilon(\boldsymbol{\eta})$ which depends on the evaluation of terms of the form $\nabla_{\boldsymbol{\eta}}\mathbf{x}^H\mathbf{h}_T(\boldsymbol{\eta})$ and $\nabla_{\boldsymbol{\eta}}\mathbf{h}_T^H(\boldsymbol{\eta})\mathbf{h}_T(\boldsymbol{\eta})$.

To elaborate, let us define by $\mathbf{G}_p(\boldsymbol{\eta}) = \frac{\partial \mathbf{Z}_E(\boldsymbol{\eta})}{\partial \eta_p} \in \mathbb{C}^{P \times P}$ the matrix obtained by evaluating the element-wise partial derivative of $\mathbf{Z}_E(\boldsymbol{\eta})$ with respect to η_p . Then, introduce:

$$\begin{aligned} d_p(\boldsymbol{\eta}) &= \frac{\partial \mathbf{x}^H\mathbf{h}_T(\boldsymbol{\eta})}{\partial \eta_p} \\ f_p(\boldsymbol{\eta}) &= \frac{\partial \mathbf{h}_T^H(\boldsymbol{\eta})\mathbf{h}_T(\boldsymbol{\eta})}{\partial \eta_p}, \end{aligned} \quad (6)$$

and the vectors $\mathbf{d}(\boldsymbol{\eta}) \in \mathbb{C}^{1 \times P}$ and $\mathbf{f}(\boldsymbol{\eta}) \in \mathbb{C}^{1 \times P}$ that contain in p -th position $d_p(\boldsymbol{\eta})$ and $f_p(\boldsymbol{\eta})$, respectively. From the Neumann series expansion of the inverse of matrices is possible to derive from (2):

$$\begin{aligned} d_p(\boldsymbol{\eta}) &= -\mathbf{x}^H\mathbf{A}\mathbf{T}(\boldsymbol{\eta})\mathbf{G}_p(\boldsymbol{\eta})\mathbf{T}(\boldsymbol{\eta})\mathbf{b} \\ f_p(\boldsymbol{\eta}) &= -2\Re\{\mathbf{h}_T^H(\boldsymbol{\eta})\mathbf{A}\mathbf{T}(\boldsymbol{\eta})\mathbf{G}_p(\boldsymbol{\eta})\mathbf{T}(\boldsymbol{\eta})\mathbf{b}\}. \end{aligned} \quad (7)$$

Due to the nonlinearity of the function $\mathbf{T}(\boldsymbol{\eta})$, the problem (5) is non-convex, and therefore it is necessary to develop a suboptimal strategy to derive a local minimum. Hence, leveraging (7), the gradient descent algorithm can be used in this case to find a local minimum of the problem. To elaborate, $\boldsymbol{\eta}$ can be adjusted iteratively according to:

$$\boldsymbol{\eta}^{(q+1)} = \boldsymbol{\eta}^{(q)} - \alpha \left[\mathbf{f}(\boldsymbol{\eta}^{(q)}) - 2\Re(\mathbf{d}(\boldsymbol{\eta}^{(q)})) \right] \quad (8)$$

where α is the learning rate. Note that the problem in (5) refers to a single input/output pair; however, due to the linearity of the gradient operator, it can be easily extended to the case of multiple inputs and multiple outputs by considering the total squared error as the sum of the individual squared errors.

A. Computational complexity

Now we consider the computational complexity of the ECO optimization problem as the complexity due to each single iteration of the gradient descent algorithm. This same quantity will then be taken into account in subsequent cases when specific SIM architectures are considered.

To begin with, it is necessary to define the complexity of calculating $\mathbf{G}_p(\boldsymbol{\eta})$ for a generic p . This complexity strongly depends on the type of network considered for connecting the ports of the ECO, specifically on whether or not there exists an easily derivable analytical formulation for $\mathbf{Z}_E(\boldsymbol{\eta})$. For example, in the case where the ECO is a classical diagonal RIS, the matrix $\mathbf{Z}_E(\boldsymbol{\eta})$ is diagonal, and each element depends on a single variable parameter, such as the phase of the reflection

coefficient of the port. In this scenario, the calculation is straightforward. In the case of BD-RIS, the calculation can be more complicated; however, if a closed-form and differentiable expression of $\mathbf{Z}_E(\boldsymbol{\eta})$ exists, the complexity of calculating $\mathbf{G}_p(\boldsymbol{\eta})$ can be neglected compared to the other calculations necessary for computing the terms $d_p(\boldsymbol{\eta})$ and $f_p(\boldsymbol{\eta})$ reported in (7). A more accurate characterization of the calculation of $\mathbf{G}_p(\boldsymbol{\eta})$ will be provided later for a specific case of SIM characterized by diagonal RIS.

To elaborate, it should be noted that the computation of $d_p(\boldsymbol{\eta})$ and $f_p(\boldsymbol{\eta})$ require to compute the inverse matrix $\mathbf{T}(\boldsymbol{\eta})$, which has a complexity of $\mathcal{O}(N^3)$. Furthermore, to evaluate the complexity of the matrix products in (7), we assume that the product of an $n \times p$ matrix by a $p \times q$ matrix requires a number of operations proportional to npq , neglecting potential optimizations from specialized algorithms for matrix multiplication. Consequently, considering that the terms in (7) need to be evaluated P times, it is easy to deduce that the overall complexity, defined as \mathcal{C}_{ECO} , is:

$$\mathcal{C}_{ECO} = \mathcal{O}(N^3) + \mathcal{O}(2PMN^2). \quad (9)$$

Note that the complexity per iteration depends both on the number of ports N of the ECO, on the number of outputs M and on the number of tunable parameters P , which can range from N , e.g., when the ECO is a diagonal RIS to N^2 for fully connected ECOs.

V. SIM MODEL

We now consider the specific case of ECO represented by a SIM. As shown in the literature, e.g., see [18]–[20], a SIM is a structure housed within a supporting framework that is surrounded by wave-absorbing materials to minimize interference from unwanted diffraction, scattering, and environmental noise. In this case, the multi-port model can be layered as shown in Fig. 2. Specifically, the SIM is composed of Q couple of facing layers, i.e., with a total of $2Q$ layers, each of which is modeled as a K port network. For simplicity, we assume that all layers are characterized by the same number of ports, but the following discussion can be easily generalized to the case where each layer has different dimensions. In this setting, the first layer receives the signal from the external environment, the second layer is connected to the first layer through an internal network, the third layer is connected to the second layer through the wireless channel, and so on, up to the last layer, which is connected to the external environment. In practice, each inner even layer, i.e., for $l = 2, 4, \dots, 2Q$, receives the signal from the previous layer through an internal network while transmitting the signal to the next layer through the wireless channel. In this scenario, the general model considered previously remains valid with a total number of ports $N = 2QK$.

Note that in [35], a multiport S-parameter model for the SIM is proposed, which, due to the equivalence between the \mathbf{S} and \mathbf{Z} matrices, is equivalent to the one presented here. In fact, an equivalent model of the SIM using S-parameters can be obtained thanks to the one-to-one relationship between the

\mathbf{S} and \mathbf{Z} matrices (see Eq. (4.44) and Eq. (4.45) in [36]). However, in our analysis, we chose to adopt the Z-parameter representation, as it allows for a more straightforward handling of situations where there is no direct connection between the ports, such as in wireless channels in the absence of line of sight (LOS) and within the internal network of the SIM. This choice also facilitates the derivation of the gradient with respect to the parameters to be optimized, which is the main goal of this work. In contrast, the authors in [35] do not develop the complete S model, asserting that understanding the role of the reconfigurable scattering matrices, i.e., the tunable parameters, within the overall transfer function is very complex. Nevertheless, we believe that the comparison between the Z and S models represents an intriguing area of investigation that deserves further exploration in future studies.

To elaborate, it is worth noting that in a SIM, each layer is only connected to two neighboring layers. As a result, the matrices \mathbf{Z}_{RE} , \mathbf{Z}_{ET} , \mathbf{Z}_{EE} , and \mathbf{Z}_E results to be very sparse. Specifically, for $\mathbf{Z}_{ET} \in \mathbb{C}^{2QK \times L}$, only the first K rows are non-zero due to the fact that only the first layer is connected to the external environment. Similarly, for $\mathbf{Z}_{RE} \in \mathbb{C}^{K \times 2QK}$, only the last K columns are non-zero. We are in particular interested in the part of the transfer function in (1) that contains the effect of the SIM, namely $\mathbf{Z}_{RE}(\mathbf{Z}_{EE} + \mathbf{Z}_E)^{-1}\mathbf{Z}_{ET}$. For convenience, we consider the matrix $\mathbf{T} = (\mathbf{Z}_{EE} + \mathbf{Z}_E)^{-1}$ as expressed by $2Q \times 2Q$ sub-matrices $\mathbf{T}_{i,j} \in \mathbb{C}^{K \times K}$, with $i = 1, \dots, 2Q$, $k = 1, \dots, 2Q$ of dimensions $K \times K$, i.e.:

$$\mathbf{T} = \begin{bmatrix} \mathbf{T}_{1,1} & \mathbf{T}_{1,2} & \cdots & \mathbf{T}_{1,2Q} \\ \mathbf{T}_{2,1} & \mathbf{T}_{2,2} & \cdots & \mathbf{T}_{2,2Q} \\ \vdots & \vdots & \ddots & \vdots \\ \mathbf{T}_{2Q,1} & \mathbf{T}_{2Q,2} & \cdots & \mathbf{T}_{2Q,2Q} \end{bmatrix} \quad (10)$$

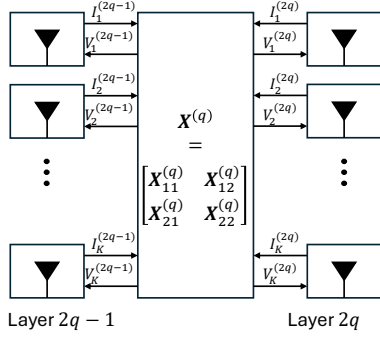
Thus, if we denote by $\mathbf{Z}'_{ET} \in \mathbb{C}^{K \times L}$ the matrix composed of the first K rows of \mathbf{Z}_{ET} , and $\mathbf{Z}'_{RE} \in \mathbb{C}^{M \times K}$, the matrix that contains the last K columns of \mathbf{Z}_{RE} , we obtain the transfer function \mathbf{H}_Z as:

$$\mathbf{H}_Z = \frac{1}{4Z_0} [\mathbf{Z}_{RT} - \mathbf{Z}'_{RE}\mathbf{T}_{2Q,1}\mathbf{Z}'_{ET}]. \quad (11)$$

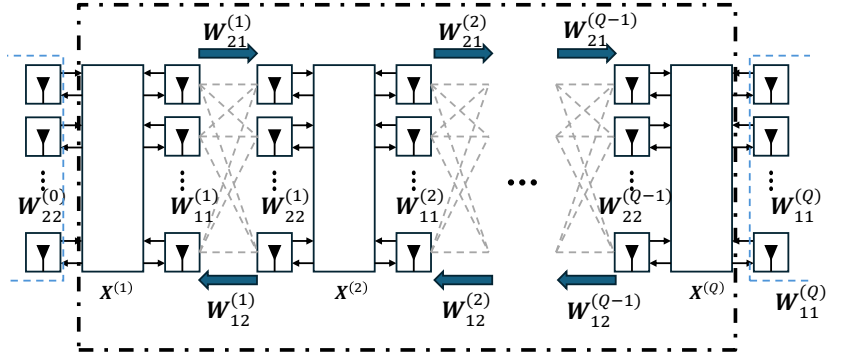
Eventually, for the SIM the transfer function in (2) can be written as:

$$\mathbf{h}_T(\boldsymbol{\eta}) = \mathbf{A}\mathbf{T}_{2Q,1}(\boldsymbol{\eta})\mathbf{b}, \quad (12)$$

where $\mathbf{A} \in \mathbb{C}^{M \times K}$ and $\mathbf{b} \in \mathbb{C}^{K \times 1}$. Regarding the matrices \mathbf{Z}_{EE} and \mathbf{Z}_E , they are band matrices that are best decomposed into sub-matrices of $K \times K$ elements. Specifically, as depicted in Fig. 2, we introduce $\mathbf{W}_{i,j}^{(q)} \in \mathbb{C}^{K \times K}$, with $q = 1, 2, \dots, Q - 1$, $i = 1, 2$, $j = 1, 2$, representing the 4 sub-matrices that characterize the connection through the wireless channel between the odd layer $2q - 1$ and the even layer $2q$. Additionally, the sub-matrix that characterizes the ports of the first layer of the SIM is denoted as $\mathbf{W}_{2,2}^{(0)} \in \mathbb{C}^{K \times K}$, and the sub-matrix that characterizes the ports of the last layer of the SIM is denoted as $\mathbf{W}_{1,1}^{(Q)} \in \mathbb{C}^{K \times K}$. The matrix \mathbf{Z}_{EE} can be



(a) Pair of facing layers.



(b) Overall model

Fig. 2: SIM model.

graphically represented as:

$$\mathbf{Z}_{EE} = \begin{bmatrix} \mathbf{W}_{2,2}^{(0)} & \mathbf{0} & \mathbf{0} & \mathbf{0} & \mathbf{0} \cdots & \mathbf{0} \\ \mathbf{0} & \mathbf{W}_{1,1}^{(1)} & \mathbf{W}_{1,2}^{(1)} & \mathbf{0} & \mathbf{0} \cdots & \mathbf{0} \\ \mathbf{0} & \mathbf{W}_{2,1}^{(1)} & \mathbf{W}_{2,2}^{(1)} & \mathbf{0} & \mathbf{0} \cdots & \mathbf{0} \\ \mathbf{0} & \mathbf{0} & \mathbf{0} & \mathbf{W}_{1,1}^{(2)} & \mathbf{W}_{1,2}^{(2)} \cdots & \mathbf{0} \\ \mathbf{0} & \mathbf{0} & \mathbf{0} & \mathbf{W}_{2,1}^{(2)} & \mathbf{W}_{2,2}^{(2)} \cdots & \mathbf{0} \\ \vdots & \vdots & \vdots & \vdots & \vdots & \vdots \\ \mathbf{0} & \mathbf{0} & \mathbf{0} & \mathbf{0} & \cdots & \mathbf{W}_{1,1}^{(Q)} \end{bmatrix} \quad (13)$$

Regarding the matrix $\mathbf{Z}_E(\boldsymbol{\eta})$, it represents the load network that in a SIM can be seen as Q separate load networks, one for each layer of the SIM. Hence, the controllable parameters independently control each layer. If we define P_q as the number of controllable parameters of layer q , with $\sum_q P_q = P$, the vector $\boldsymbol{\eta}$ can be appropriately written as $\boldsymbol{\eta} = \{\boldsymbol{\eta}_1, \dots, \boldsymbol{\eta}_Q\}$, where $\boldsymbol{\eta}_q = \{\eta_{q,1}, \dots, \eta_{q,P_q}\}$. We can then introduce the matrices $\mathbf{X}_{i,j}^{(q)}(\boldsymbol{\eta}_q) \in \mathbb{C}^{K \times K}$, with $q = 1, 2, \dots, Q$, $i = 1, 2$, $j = 1, 2$, which represent the 4 Z matrices of the connection in the load network between layer $2q-1$ and layer $2q$. Omitting the dependence of $\mathbf{X}_{i,j}^{(q)}$ on $\boldsymbol{\eta}_q$ for ease of representation, the matrix $\mathbf{Z}_E(\boldsymbol{\eta})$ can thus be written as:

$$\mathbf{Z}_E(\boldsymbol{\eta}) = \begin{bmatrix} \mathbf{X}_{1,1}^{(1)} & \mathbf{X}_{1,2}^{(1)} & \mathbf{0} & \mathbf{0} \cdots & \mathbf{0} & \mathbf{0} \\ \mathbf{X}_{2,1}^{(1)} & \mathbf{X}_{2,2}^{(1)} & \mathbf{0} & \mathbf{0} \cdots & \mathbf{0} & \mathbf{0} \\ \mathbf{0} & \mathbf{0} & \mathbf{X}_{1,1}^{(2)} & \mathbf{X}_{1,2}^{(2)} \cdots & \mathbf{0} & \mathbf{0} \\ \mathbf{0} & \mathbf{0} & \mathbf{X}_{2,1}^{(2)} & \mathbf{X}_{2,2}^{(2)} \cdots & \mathbf{0} & \mathbf{0} \\ \vdots & \vdots & \vdots & \vdots & \vdots & \vdots \\ \mathbf{0} & \mathbf{0} & \mathbf{0} & \mathbf{0} & \mathbf{X}_{1,1}^{(Q)} & \mathbf{X}_{1,2}^{(Q)} \\ \mathbf{0} & \mathbf{0} & \mathbf{0} & \mathbf{0} & \mathbf{X}_{2,1}^{(Q)} & \mathbf{X}_{2,2}^{(Q)} \end{bmatrix} \quad (14)$$

Given the band structure of the matrices \mathbf{Z}_{EE} and \mathbf{Z}_E , it is possible to derive an iterative approach for the calculation of the inverse $\mathbf{T}(\boldsymbol{\eta}) = (\mathbf{Z}_{EE} + \mathbf{Z}_E(\boldsymbol{\eta}))^{-1}$ that has reduced complexity compared to $\mathcal{O}(N^3)$. This aspect is not further addressed in this work, referring the reader to specific literature on the inversion of band matrices.

A. Gradients evaluation for a SIM

Based on the above, the expression of the gradients given in (7) can also be significantly simplified. To elaborate, let us denote by $\mathbf{Z}_E^{(q)}(\boldsymbol{\eta}_q) = \{\mathbf{X}_{i,j}^{(q)}\} \in \mathbb{C}^{2K \times 2K}$ the matrix containing the q -th block of $\mathbf{Z}_E(\boldsymbol{\eta})$ and by $\mathbf{G}_{q,p}(\boldsymbol{\eta}_q) = \frac{\partial \mathbf{Z}_E^{(q)}(\boldsymbol{\eta}_q)}{\partial \eta_{q,p}} \in \mathbb{C}^{2K \times 2K}$ the matrix obtained by evaluating the element-wise partial derivative of $\mathbf{Z}_E^{(q)}(\boldsymbol{\eta}_q)$ with respect to $\eta_{q,p}$. Then, we introduce:

$$\begin{aligned} d_{q,p}(\boldsymbol{\eta}) &= \frac{\partial \mathbf{x}^H \mathbf{h}_T(\boldsymbol{\eta})}{\partial \eta_{q,p}} \\ f_{q,p}(\boldsymbol{\eta}) &= \frac{\partial \mathbf{h}_T^H(\boldsymbol{\eta}) \mathbf{h}_T(\boldsymbol{\eta})}{\partial \eta_{q,p}}. \end{aligned} \quad (15)$$

Hence, denoting by $\mathbf{R}_q(\boldsymbol{\eta}) = \{\mathbf{T}_{2Q,2q-1}(\boldsymbol{\eta}), \mathbf{T}_{2Q,2q}(\boldsymbol{\eta})\} \in \mathbb{C}^{K \times 2K}$, and $\mathbf{S}_q(\boldsymbol{\eta}) = \{\mathbf{T}_{2q-1,1}^T(\boldsymbol{\eta}), \mathbf{T}_{2q,1}^T(\boldsymbol{\eta})\}^T \in \mathbb{C}^{2K \times K}$, it is straightforward to get:

$$\begin{aligned} d_{q,p}(\boldsymbol{\eta}) &= -\mathbf{x}^H \mathbf{A} \mathbf{R}_q(\boldsymbol{\eta}) \mathbf{G}_{q,p}(\boldsymbol{\eta}_q) \mathbf{S}_q(\boldsymbol{\eta}) \mathbf{b} \\ f_{q,p}(\boldsymbol{\eta}) &= -2\Re \{ \mathbf{h}_T^H(\boldsymbol{\eta}) \mathbf{A} \mathbf{R}_q(\boldsymbol{\eta}) \mathbf{G}_{q,p}(\boldsymbol{\eta}_q) \mathbf{S}_q(\boldsymbol{\eta}) \mathbf{b} \}. \end{aligned} \quad (16)$$

The particular layered structure of the SIM allows for a reduction in computational complexity compared to the generic ECO case. To elaborate, considering that in this case $\mathbf{A} \in \mathbb{C}^{M \times K}$, similarly to the ECO case, we can derive:

$$\mathcal{C}_{SIM} = \mathcal{O}(N^3) + \mathcal{O}(6PMK^2), \quad (17)$$

where, as commented above, in (17) we have considered the worst-case scenario in which the calculation of $\mathbf{T}(\boldsymbol{\eta})$ occurs with complexity $\mathcal{O}(N^3)$, that is, not considering the possibility of leveraging the band structure of the involved matrices.

B. SIM with diagonal RISs

When the faced layers of the SIM are composed of diagonal RISs [35], each load network element of layer $2q-1$ of the SIM is connected to a single element of layer $2q$. Hence, the load network can be decomposed into K two-ports networks $\mathbf{D}_k^{(q)} \in \mathbb{C}^{2 \times 2}$ with elements $D_k^{(q)}(n, m)$ for $n = 1, 2$ and $m =$

1, 2. In this setting, the matrices $\mathbf{X}_{n,m}^{(q)}$ in (14) are shown to be diagonal matrices containing the element $D_k^{(q)}(n, m)$ in the k -th diagonal entry:

$$\mathbf{X}_{n,m}^{(q)} = \begin{bmatrix} D_1^{(q)}(n, m) & 0 & \cdots & 0 \\ 0 & D_2^{(q)}(n, m) & \cdots & 0 \\ \vdots & \vdots & \ddots & \vdots \\ 0 & 0 & \cdots & D_K^{(q)}(n, m) \end{bmatrix} \quad (18)$$

Since in a SIM each layer operates in transmissive mode, the two-port network $D_p^{(q)}(n, m)$, $p = 1, \dots, K$, can be characterized by a single tunable parameter $\eta_{q,p}$, representing the transmission coefficient angle [35], i.e., in this case $P_q = K$ and $P = QK$. Representing as in [35] the network in S-parameters, we obtain a network where the diagonal elements $s_{1,1}$ and $s_{2,2}$ are zero, while $s_{2,1} = s_{1,2} = e^{j\eta_{q,p}}$. In the Z-parameter representation, we then have [36]:

$$\mathbf{D}_p^{(q)} = jZ_0 \begin{bmatrix} \frac{\cos(\eta_{q,p})}{\sin(\eta_{q,p})} & \frac{1}{\sin(\eta_{q,p})} \\ \frac{1}{\sin(\eta_{q,p})} & \frac{\cos(\eta_{q,p})}{\sin(\eta_{q,p})} \end{bmatrix}. \quad (19)$$

Denoting $\mathbf{D}_p^{\prime(q)} = \frac{\partial \mathbf{D}_p^{(q)}}{\partial \eta_{q,p}} \in \mathbb{C}^{2 \times 2}$, we have:

$$\mathbf{D}_p^{\prime(q)} = -jZ_0 \begin{bmatrix} \left(\frac{\cos(\eta_{q,p})}{\sin(\eta_{q,p})} \right)^2 + 1 & \frac{\cos(\eta_{q,p})}{\sin^2(\eta_{q,p})} \\ \frac{\cos(\eta_{q,p})}{\sin^2(\eta_{q,p})} & \left(\frac{\cos(\eta_{q,p})}{\sin(\eta_{q,p})} \right)^2 + 1 \end{bmatrix}. \quad (20)$$

It is then straightforward to observe that $\mathbf{G}_{p,q}(\eta_q) = \mathbf{G}_{p,q}(\eta_{q,p})$, i.e., $\mathbf{G}_{p,q}$ is a function of $\eta_{q,p}$ only. Hence, if we introduce the element-selection diagonal matrices $\mathbf{J}_p \in \mathbb{C}^{K \times K}$ consisting of all zeros except in the p -th diagonal element, which is one, we easily get:

$$\mathbf{G}_{p,q}(\eta_{q,p}) \begin{bmatrix} D_p^{\prime(q)}(1,1)\mathbf{J}_p & D_p^{\prime(q)}(1,2)\mathbf{J}_p \\ D_p^{\prime(q)}(2,1)\mathbf{J}_p & D_p^{\prime(q)}(2,2)\mathbf{J}_p \end{bmatrix}. \quad (21)$$

Therefore, the expression of the gradients in (16) can also be simplified. To this end, we introduce the vectors $\mathbf{t}_{q,p}^{(1)}(\boldsymbol{\eta}) \in \mathbb{C}^{K \times 1}$ and $\mathbf{t}_{q,p}^{(2)}(\boldsymbol{\eta}) \in \mathbb{C}^{K \times 1}$ as the p -th columns of the matrices $\mathbf{T}_{2Q,2q-1}(\boldsymbol{\eta})$ and $\mathbf{T}_{2Q,2q}(\boldsymbol{\eta})$, respectively. Similarly, we introduce the vectors $\mathbf{t}_{q,p}^{(3)}(\boldsymbol{\eta}) \in \mathbb{C}^{1 \times K}$ and $\mathbf{t}_{q,p}^{(4)}(\boldsymbol{\eta}) \in \mathbb{C}^{1 \times K}$ as the p -th rows of the matrices $\mathbf{T}_{2q-1,1}(\boldsymbol{\eta})$ and $\mathbf{T}_{2q,1}(\boldsymbol{\eta})$, respectively. Therefore, introducing $\mathbf{F}_{q,p}$ defined in (22), we get:

$$\begin{aligned} d_{q,p}(\boldsymbol{\eta}) &= -\mathbf{x}^H \mathbf{A} \mathbf{F}_{q,p}(\boldsymbol{\eta}) \mathbf{b} \\ f_{q,p}(\boldsymbol{\eta}) &= -2\Re \{ \mathbf{h}_T^H(\boldsymbol{\eta}) \mathbf{A} \mathbf{F}_{q,p}(\boldsymbol{\eta}) \mathbf{b} \}. \end{aligned} \quad (23)$$

Hence, a diagonal SIM allows for a reduction in complexity due to the simplification of gradient calculation. To elaborate, considering that to calculate (22) for each p there is a complexity of $\mathcal{O}(4PK)$, it is easy to derive from (23) the complexity of diagonal SIM, denoted by \mathcal{C}_{D-SIM} , as:

$$\mathcal{C}_{D-SIM} = \mathcal{O}(N^3) + \mathcal{O}(PMK^2). \quad (24)$$

C. Unilateral approximation

In [35], it is shown that the model used in all the works addressing SIM so far relies on various approximations, including the unilateral approximation. Essentially, this approximation consists of assuming that the interaction between two layers of the SIM occurs in one direction only, meaning that the wireless channel separating two SIMs is not reciprocal. In this case, we have $\mathbf{W}_{1,2}^{(q)} = \mathbf{0}$, $\forall q$, in the expression of \mathbf{Z}_{EE} reported in (13). Let us omit for the sake of notations the dependence on $\boldsymbol{\eta}$ of all the involved matrices. Since $\mathbf{T}(\mathbf{Z}_{EE} + \mathbf{Z}_E) = \mathbf{I}$, we have from (13) and (14):

$$\begin{aligned} \mathbf{T}_{2Q,2Q-1} \mathbf{X}_{1,2}^{(Q)} + \mathbf{T}_{2Q,2Q} (\mathbf{X}_{2,2}^{(Q)} + \mathbf{W}_{1,1}^{(Q)}) &= \mathbf{I} \\ \mathbf{T}_{2Q,2Q-1} (\mathbf{X}_{1,1}^{(Q)} + \mathbf{W}_{2,2}^{(Q-1)}) + \mathbf{T}_{2Q,2Q} \mathbf{X}_{2,1}^{(Q)} &= \mathbf{0}. \end{aligned} \quad (25)$$

Introducing

$$\boldsymbol{\Omega}_q = \left(\mathbf{X}_{2,2}^{(q)} + \mathbf{W}_{1,1}^{(q)} - \mathbf{X}_{2,1}^{(q)} (\mathbf{X}_{1,1}^{(q)} + \mathbf{W}_{2,2}^{(q-1)})^{-1} \mathbf{X}_{1,2}^{(q)} \right)^{-1}, \quad (26)$$

from (25) we have:

$$\mathbf{T}_{2Q,2Q} = \boldsymbol{\Omega}_Q. \quad (27)$$

Then, it is easy to derive the following relationships for $q = Q, Q-1, \dots, 2$:

$$\mathbf{T}_{2Q,2q-1} = -\mathbf{T}_{2Q,2q} \mathbf{X}_{2,1}^{(q)} (\mathbf{X}_{1,1}^{(q)} + \mathbf{W}_{2,2}^{(q-1)})^{-1} \quad (28)$$

$$\mathbf{T}_{2Q,2q-2} = -\mathbf{T}_{2Q,2q-1} \mathbf{W}_{2,1}^{(q-1)} \boldsymbol{\Omega}_{q-1},$$

and

$$\mathbf{T}_{2Q,1} = -\mathbf{T}_{2Q,2} \mathbf{X}_{2,1}^{(1)} (\mathbf{X}_{1,1}^{(1)} + \mathbf{W}_{2,2}^{(0)})^{-1}. \quad (29)$$

The relationships obtained in (26), (27), (28) and (29) enable the iterative calculation of all the terms $\mathbf{T}_{2Q,q}$ for $q = 1, 2, \dots, 2Q$ of the matrix \mathbf{T} . Consequently, the transfer function $\mathbf{h}_T(\boldsymbol{\eta})$ in (12), which depends on $\mathbf{T}_{2Q,1}$, can be evaluated without the need to compute the inverse of the large matrix $\mathbf{Z}_{EE} + \mathbf{Z}_E$.

From the relation $(\mathbf{Z}_{EE} + \mathbf{Z}_E) \mathbf{T} = \mathbf{I}$, it is possible to derive a similar set of equations concerning the first column $\mathbf{T}_{q,1}$. To elaborate, introducing:

$$\boldsymbol{\zeta}_q = \left(\mathbf{X}_{1,1}^{(q)} + \mathbf{W}_{2,2}^{(q-1)} - \mathbf{X}_{1,2}^{(q)} (\mathbf{X}_{2,2}^{(q)} + \mathbf{W}_{2,2}^{(q-1)})^{-1} \mathbf{X}_{2,1}^{(q)} \right)^{-1}, \quad (30)$$

we have:

$$\mathbf{T}_{1,1} = \boldsymbol{\zeta}_1, \quad (31)$$

and for $q = 1, 2, \dots, Q-1$:

$$\mathbf{T}_{2q,1} = - \left(\mathbf{X}_{2,2}^{(q)} + \mathbf{W}_{1,1}^{(q)} \right)^{-1} \mathbf{X}_{2,1}^{(q)} \mathbf{T}_{2q-1,1} \quad (32)$$

$$\mathbf{T}_{2q+1,1} = -\boldsymbol{\zeta}_{q+1} \mathbf{W}_{2,1}^{(q)} \mathbf{T}_{2q,1}.$$

Note that the ability to calculate the matrices $\mathbf{T}_{2Q,q}$ and $\mathbf{T}_{q,1}$, for $q = 1, \dots, Q$ in an iterative manner also simplifies the computation of the gradients in (16) and (23). Specifically,

$$\mathbf{F}_{q,p}(\boldsymbol{\eta}) = \left(D_p^{(q)}(1,1)\mathbf{t}_{q,p}^{(1)}(\boldsymbol{\eta}) + D_p^{(q)}(2,1)\mathbf{t}_{q,p}^{(2)}(\boldsymbol{\eta}) \right) \mathbf{t}_{q,p}^{(3)}(\boldsymbol{\eta}) + \left(D_p^{(q)}(1,2)\mathbf{t}_{q,p}^{(1)}(\boldsymbol{\eta}) + D_p^{(q)}(2,2)\mathbf{t}_{q,p}^{(2)}(\boldsymbol{\eta}) \right) \mathbf{t}_{q,p}^{(4)}(\boldsymbol{\eta}) \quad (22)$$

compared to the *SIM* case, calculating $\mathbf{R}_{q,p}(\boldsymbol{\eta})$ and $\mathbf{S}_{q,p}(\boldsymbol{\eta})$ requires only the two iterative procedures listed in (25)-(32), each with a complexity of $\mathcal{O}(3QK^3)$. Similarly, compared to the *D-SIM* case in (24), calculating $\mathbf{F}_{q,p}(\boldsymbol{\eta})$ also requires a complexity of $\mathcal{O}(3QK^3)$. Therefore, denoting by *CU-SIM* the complexity of the *SIM* with unilateral approximation, we have:

$$\mathcal{C}_{U-SIM} = \mathcal{O}(6QK^3) + \mathcal{O}(6PMK^2). \quad (33)$$

while denoting by \mathcal{C}_{DU-SIM} the complexity in the case of unilateral approximation with diagonal RIS, denoted as *DU-SIM*, we have:

$$\mathcal{C}_{DU-SIM} = \mathcal{O}(6QK^3) + \mathcal{O}(PMK^2). \quad (34)$$

D. Unilateral approximation with diagonal and ideal RISs

In the case of ideal *SIMs*, we assume that there is no coupling between the elements of the *RISs* that compose them. We also assume that the matrices $\mathbf{W}_{1,1}^{(q)}$ and $\mathbf{W}_{2,2}^{(q-1)}$ are characterized by impedances at the ports Z_0 . Specifically, we have $\mathbf{W}_{1,1}^{(q)} = \mathbf{W}_{2,2}^{(q-1)} = Z_0 \mathbf{I}_K$. Under these conditions, it follows that the matrices $\boldsymbol{\Omega}_q$ in (27) are diagonal. Moreover, from (19), and denoting $\eta = \eta_{q,p}$, each diagonal element $\omega_{q,p}$ of $\boldsymbol{\Omega}_q$ takes the form:

$$\begin{aligned} \omega_{q,p} &= \frac{1}{Z_0} \left(1 + j \frac{\cos \eta}{\sin \eta} - j \frac{1}{\sin \eta} \left(1 + j \frac{\cos \eta}{\sin \eta} \right)^{-1} j \frac{1}{\sin \eta} \right)^{-1} \\ &= \frac{1}{Z_0} \left(\frac{\sin \eta + j \cos \eta}{\sin \eta} + \frac{1}{\sin \eta (\sin \eta + j \cos \eta)} \right)^{-1} \\ &= \frac{1}{Z_0} \left(\frac{\sin^2 \eta - \cos^2 \eta + 2j \cos \eta \sin \eta + 1}{\sin \eta (\sin \eta + j \cos \eta)} \right)^{-1} \\ &= \frac{1}{2Z_0}. \end{aligned} \quad (35)$$

It is easy to verify with similar steps that ζ_q is diagonal with the p -th entry equal to $\zeta_{q,p} = \frac{1}{2Z_0}$. Furthermore, the matrix $\mathbf{X}_{2,1}^{(q)} \left(\mathbf{X}_{1,1}^{(q)} + \mathbf{W}_{2,2}^{(q-1)} \right)^{-1}$ that appears in (28) is also diagonal. Let us denote this matrix by \mathbf{Y}_q with $Y_{q,p}$ representing its p -th entry. We have:

$$\begin{aligned} Y_{q,p} &= j \frac{1}{\sin \eta_{q,p}} \left(1 + j \frac{\cos \eta_{q,p}}{\sin \eta_{q,p}} \right)^{-1} \\ &= e^{j\eta_{q,p}}. \end{aligned} \quad (36)$$

For the sake of notation, we denote by $\mathbf{Y}_q = e^{j\boldsymbol{\eta}_q}$. From (26), (27), (28) and (29), setting $\mathbf{W}_{2,1}^{(Q)} = \mathbf{I}_K$, we can derive:

$$\mathbf{T}_{2Q,1} = \left(-\frac{1}{2Z_0} \right)^Q e^{j\boldsymbol{\eta}_Q} \prod_{q=Q-1, Q-2, \dots, 1} \mathbf{W}_{2,1}^{(q)} e^{j\boldsymbol{\eta}_q}. \quad (37)$$

It is noted from (12) that (37) represents the *I/O* relationship of the *SIM*, which becomes a cascade comprising the propagation through the channels that separate the levels $2q$ and $2q+1$, represented by the terms $\frac{1}{2Z_0} \mathbf{W}_{2,1}^{(q)}$, along with the phase shifts introduced during the transition from level $2q-1$ to level $2q$. In this particular case, therefore, the *SIM* model coincides with that traditionally used in all previous works, e.g., see [18]–[22], [30]–[34].

It should be noted that in the models used to characterize the *SIM* thus far, the terms $\frac{1}{2Z_0} \mathbf{W}_{2,1}^{(q)}$ have been modeled using the Rayleigh-Sommerfeld diffraction equation [37], which has been applied in the context of all-optical diffractive deep neural networks (*D2NN*). However, its application to *SIMs* operating at radio frequencies may be questionable. With the proposed model with parameters \mathbf{Z} , it more generally represents the coupling in terms of voltage to current between the ports of two *RIS* at different levels of the *SIM*.

The assumption of unidirectionality facilitates the simplification of the gradient calculation. In this context, as demonstrated in previous works that consider the ideal *SIM* model with unidirectional approximation, which we refer to here as *DU-SIM_{id}*, the gradient with respect to the phase shifts $\boldsymbol{\eta}_q$ can be computed using an iterative relationship similar to the one shown in (37). Specifically, it is straightforward to derive the complexity for calculating the gradient with respect to all the phase shifts as:

$$\mathcal{C}_{DU-SIM_{id}} = \mathcal{O}(4Q^2K^2). \quad (38)$$

The computation in (38) stems from the fact that, as shown in [18], [20], each gradient element requires calculating a transfer function, whose complexity matches that of the transfer function in (12). With the iterative approach in (37), this complexity is $\mathcal{O}(2QK^2)$. Since the number of gradient vectors to be computed is $2Q$, we arrive at the expression in (38).

1) *Gradient computation through back propagation:* We introduce $\mathbf{I}_q \in \mathbb{C}^{K \times 1}$ and $\mathbf{O}_q \in \mathbb{C}^{K \times 1}$ as:

$$\begin{aligned} \mathbf{O}_q &= -\frac{1}{2Z_0} e^{j\boldsymbol{\eta}_q} \mathbf{I}_q \quad \text{for } q = 1, \dots, Q \\ \mathbf{I}_q &= \mathbf{W}_{2,1}^{(q)} \mathbf{O}_{q-1} \quad \text{for } q = 2, \dots, Q \\ \mathbf{I}_1 &= \mathbf{b} \end{aligned} \quad (39)$$

so that it is easy to get from (37) $\mathbf{T}_{2Q,1} = \mathbf{O}_Q$. Accordingly, the error in (3) can be written as:

$$\epsilon = (\mathbf{A}\mathbf{O}_Q - \mathbf{x})^H (\mathbf{A}\mathbf{O}_Q - \mathbf{x}). \quad (40)$$

We have:

$$\boldsymbol{\lambda}_Q = \frac{\partial \epsilon}{\partial \mathbf{O}_Q} = \mathbf{A}^H (\mathbf{A}\mathbf{O}_Q - \mathbf{x}). \quad (41)$$

From the definitions in (39), it is easy to find the iterative relationship:

$$\lambda_{q-1} = \frac{\partial \epsilon}{\partial \mathbf{O}_{q-1}} = -\frac{1}{2Z_0} \left[e^{j\eta_q} \mathbf{W}_{2,1}^{(q)} \right]^H \lambda_q, \quad (42)$$

for $q = 2, \dots, Q$. Hence, the terms λ_q can be evaluated iteratively from λ_Q following the backward propagation algorithm (42). From (39) and (42), denoting by $\mu_q = \frac{\partial \epsilon}{\partial \eta_q}$ we have:

$$\begin{aligned} \mu_q &= \Re \left[\left(\frac{\partial \mathbf{O}_q}{\partial \eta} \right)^H \frac{\partial \epsilon}{\partial \mathbf{O}_q} \right] \\ &= -\frac{1}{2Z_0} \Re \left[\left(j e^{j\eta_q} \mathbf{I}_q \right)^H \text{diag}(\lambda_q) \right]. \end{aligned} \quad (43)$$

The use of a back-propagation algorithm for gradient calculation allows for a further reduction in complexity with respect to (38). In fact, the calculation of the terms λ_q can be performed from Q backward to index 1 with a complexity of $\mathcal{O}(2QK^2)$ after computing the terms in (39) with forward propagation, which also requires a complexity of $\mathcal{O}(2QK^2)$. This approach closely resembles the backpropagation algorithm used in a classic neural networks, although the architecture is quite different here, as the tunable parameters are not in the weights of the channel $\mathbf{W}_{2,1}^{(q)}$, but rather in the phase shifts introduced at each node. To summarize, for the case of $DU - SIM_{id}$ model with back propagation, referred to as $DU - SIM_{id,bp}$ we have:

$$\mathcal{C}_{DU-SIM_{id,bp}} = \mathcal{O}(4QK^2). \quad (44)$$

VI. CONCLUSION

In this work, we have introduced a comprehensive multiport network model for the optimization of SIMs. In particular, by situating our approach within the context of a general Electromagnetic Collaborative Object (ECO), we have established a foundational Z-parameter model that allows for the investigation of SIM architectures without relying on limiting assumptions, such as unilateral approximations or the absence of mutual coupling. Our proposed framework facilitates broader applicability and provides deeper insights into SIM optimization across various configurations. We have emphasized the impact of commonly used assumptions on model performance and potential simplifications, illustrating how variations in these assumptions can affect the complexity of the problem. As a further contribution, we have proposed a backpropagation algorithm for implementing the gradient descent method for a simplified SIM configuration.

REFERENCES

[1] M. D. Renzo, M. Debbah, D. T. P. Huy, A. Zappone, M. Alouini, C. Yuen, V. Sciancalepore, G. C. Alexandropoulos, J. Hoydis, H. Gacanin, J. de Rosny, A. Bounceur, G. Lerosey, and M. Fink, "Smart radio environments empowered by reconfigurable AI metasurfaces: an idea whose time has come," *EURASIP J. Wirel. Commun. Netw.*, vol. 2019, p. 129, 2019. [Online]. Available: <https://doi.org/10.1186/s13638-019-1438-9>

[2] Q. Wu, S. Zhang, B. Zheng, C. You, and R. Zhang, "Intelligent reflecting surface-aided wireless communications: A tutorial," *IEEE Transactions on Communications*, vol. 69, no. 5, pp. 3313–3351, 2021.

[3] M. Di Renzo, A. Zappone, M. Debbah, M.-S. Alouini, C. Yuen, J. de Rosny, and S. Tretyakov, "Smart radio environments empowered by reconfigurable intelligent surfaces: How it works, state of research, and the road ahead," *IEEE Journal on Selected Areas in Communications*, vol. 38, no. 11, pp. 2450–2525, 2020.

[4] M. Di Renzo, F. H. Danufane, and S. Tretyakov, "Communication models for reconfigurable intelligent surfaces: From surface electromagnetics to wireless networks optimization," *Proceedings of the IEEE*, vol. 110, no. 9, pp. 1164–1209, 2022.

[5] S. Abeywickrama, R. Zhang, Q. Wu, and C. Yuen, "Intelligent reflecting surface: Practical phase shift model and beamforming optimization," *IEEE Transactions on Communications*, vol. 68, no. 9, pp. 5849–5863, 2020.

[6] A. Rafique, N. Ul Hassan, M. Zubair, I. H. Naqvi, M. Q. Mehmood, M. D. Renzo, M. Debbah, and C. Yuen, "Reconfigurable intelligent surfaces: Interplay of unit cell and surface-level design and performance under quantifiable benchmarks," *IEEE Open Journal of the Communications Society*, vol. 4, pp. 1583–1599, 2023.

[7] M. T. Ivrlač and J. A. Nossek, "Toward a circuit theory of communication," *IEEE Transactions on Circuits and Systems I: Regular Papers*, vol. 57, no. 7, pp. 1663–1683, 2010.

[8] G. Gradoni and M. Di Renzo, "End-to-end mutual coupling aware communication model for reconfigurable intelligent surfaces: An electromagnetic-compliant approach based on mutual impedances," *IEEE Wireless Communications Letters*, vol. 10, no. 5, pp. 938–942, 2021.

[9] X. Qian and M. D. Renzo, "Mutual coupling and unit cell aware optimization for reconfigurable intelligent surfaces," *IEEE Wireless Communications Letters*, vol. 10, no. 6, pp. 1183–1187, 2021.

[10] A. Abrardo, D. Dardari, M. Di Renzo, and X. Qian, "Mimo interference channels assisted by reconfigurable intelligent surfaces: Mutual coupling aware sum-rate optimization based on a mutual impedance channel model," *IEEE Wireless Communications Letters*, vol. 10, no. 12, pp. 2624–2628, 2021.

[11] M. Di Renzo, A. Zappone, M. Debbah, M.-S. Alouini, C. Yuen, J. de Rosny, and S. Tretyakov, "Smart radio environments empowered by reconfigurable intelligent surfaces: How it works, state of research, and the road ahead," *IEEE Journal on Selected Areas in Communications*, vol. 38, no. 11, pp. 2450–2525, 2020.

[12] M. Movahediqomi, G. Ptitcyn, and S. Tretyakov, "Comparison between different designs and realizations of anomalous reflectors for extreme deflections," *IEEE Transactions on Antennas and Propagation*, vol. 71, no. 10, pp. 8007–8017, 2023.

[13] A. Abrardo, A. Toccafondi, and M. D. Renzo, "Analysis and optimization of reconfigurable intelligent surfaces based on s-parameters multiport network theory," *arXiv:2308.16856 [cs.IT]*, accepted in *IEEE EUCAP 2024*, August 2023.

[14] A. Abrardo, A. Toccafondi, and M. Di Renzo, "Design of reconfigurable intelligent surfaces by using s-parameter multiport network theory—optimization and full-wave validation," *IEEE Transactions on Wireless Communications*, vol. 23, no. 11, pp. 17 084–17 102, 2024.

[15] M. Nerini, S. Shen, and B. Clerckx, "Closed-form global optimization of beyond diagonal reconfigurable intelligent surfaces," *IEEE Trans. Wirel. Commun.*, vol. 23, no. 2, pp. 2311–2324, 2024.

[16] H. Li, S. Shen, and B. Clerckx, "Beyond diagonal reconfigurable intelligent surfaces: From transmitting and reflecting modes to single-, group-, and fully-connected architectures," *IEEE Transactions on Wireless Communications*, vol. 22, no. 4, pp. 2311–2324, 2023.

[17] C. Liu, Q. Ma, Z. J. Luo, Q. R. Hong, Q. Xiao, H. C. Zhang, L. Miao, W. M. Yu, Q. Cheng, L. Li, and T. J. Cui, "A programmable diffractive deep neural network based on a digital-coding metasurface array," *Nat. Electron.*, vol. 5, no. 2, pp. 113–122, 2022. [Online]. Available: <https://doi.org/10.1038/s41928-022-00719-9>

[18] J. An, C. Xu, D. W. K. Ng, G. C. Alexandropoulos, C. Huang, C. Yuen, and L. Hanzo, "Stacked intelligent metasurfaces for efficient holographic MIMO communications in 6g," *IEEE J. Sel. Areas Commun.*, vol. 41, no. 8, pp. 2380–2396, 2023. [Online]. Available: <https://doi.org/10.1109/JSAC.2023.3288261>

[19] N. U. Hassan, J. An, M. D. Renzo, M. Debbah, and C. Yuen, "Efficient beamforming and radiation pattern control using stacked intelligent metasurfaces," *IEEE Open J. Commun. Soc.*, vol. 5, pp. 599–611, 2024. [Online]. Available: <https://doi.org/10.1109/OJCOMS.2023.3349155>

- [20] J. An, C. Yuen, C. Xu, H. Li, D. W. K. Ng, M. D. Renzo, M. Debbah, and L. Hanzo, "Stacked intelligent metasurface-aided MIMO transceiver design," *IEEE Wirel. Commun.*, vol. 31, no. 4, pp. 123–131, 2024. [Online]. Available: <https://doi.org/10.1109/MWC.013.2300259>
- [21] E. Basar, G. C. Alexandropoulos, Y. Liu, Q. Wu, S. Jin, C. Yuen, O. A. Dobre, and R. Schober, "Reconfigurable intelligent surfaces for 6g: Emerging hardware architectures, applications, and open challenges," *IEEE Veh. Technol. Mag.*, vol. 19, no. 3, pp. 27–47, 2024. [Online]. Available: <https://doi.org/10.1109/MVT.2024.3415570>
- [22] J. An, M. D. Renzo, M. Debbah, and C. Yuen, "Stacked intelligent metasurfaces for multiuser beamforming in the wave domain," in *IEEE International Conference on Communications, ICC 2023, Rome, Italy, May 28 - June 1, 2023*. IEEE, 2023, pp. 2834–2839. [Online]. Available: <https://doi.org/10.1109/ICC45041.2023.10279173>
- [23] A. K. Papazafeiropoulos, P. Kourtessis, S. Chatzinotas, D. I. Kaklamani, and I. S. Venieris, "Achievable rate optimization for large stacked intelligent metasurfaces based on statistical CSI," *IEEE Wirel. Commun. Lett.*, vol. 13, no. 9, pp. 2337–2341, 2024. [Online]. Available: <https://doi.org/10.1109/LWC.2024.3407863>
- [24] H. Liu, J. An, D. W. K. Ng, G. C. Alexandropoulos, and L. Gan, "Drl-based orchestration of multi-user MISO systems with stacked intelligent metasurfaces," in *IEEE International Conference on Communications, ICC 2024, Denver, CO, USA, June 9-13, 2024*. IEEE, 2024, pp. 4991–4996. [Online]. Available: <https://doi.org/10.1109/ICC51166.2024.10622385>
- [25] Y. Hu, J. Zhang, E. Shi, Y. Lu, J. An, C. Yuen, and B. Ai, "Joint beamforming and power allocation design for stacked intelligent metasurfaces-aided cell-free massive mimo systems," *IEEE Transactions on Vehicular Technology*, pp. 1–6, 2024.
- [26] Q. Li, M. El-Hajjar, C. Xu, J. An, C. Yuen, and L. Hanzo, "Stacked intelligent metasurfaces for holographic mimo-aided cell-free networks," *IEEE Trans. Commun.*, vol. 72, no. 11, pp. 7139–7151, 2024. [Online]. Available: <https://doi.org/10.1109/TCOMM.2024.3403499>
- [27] S. Lin, J. An, L. Gan, M. Debbah, and C. Yuen, "Stacked intelligent metasurface enabled LEO satellite communications relying on statistical CSI," *IEEE Wirel. Commun. Lett.*, vol. 13, no. 5, pp. 1295–1299, 2024. [Online]. Available: <https://doi.org/10.1109/LWC.2024.3368238>
- [28] A. K. Papazafeiropoulos, P. Kourtessis, S. Chatzinotas, D. I. Kaklamani, and I. S. Venieris, "Near-field beamforming for stacked intelligent metasurfaces-assisted MIMO networks," *IEEE Wirel. Commun. Lett.*, vol. 13, no. 11, pp. 3035–3039, 2024. [Online]. Available: <https://doi.org/10.1109/LWC.2024.3438840>
- [29] X. Jia, J. An, H. Liu, L. Gan, M. D. Renzo, M. Debbah, and C. Yuen, "Stacked intelligent metasurface enabled near-field multiuser beamforming in the wave domain," in *99th IEEE Vehicular Technology Conference, VTC Spring 2024, Singapore, June 24-27, 2024*. IEEE, 2024, pp. 1–5. [Online]. Available: <https://doi.org/10.1109/VTC2024-Spring62846.2024.10683447>
- [30] J. An, C. Yuen, Y. L. Guan, M. D. Renzo, M. Debbah, H. V. Poor, and L. Hanzo, "Stacked intelligent metasurface performs a 2d DFT in the wave domain for DOA estimation," in *IEEE International Conference on Communications, ICC 2024, Denver, CO, USA, June 9-13, 2024*. IEEE, 2024, pp. 3445–3451. [Online]. Available: <https://doi.org/10.1109/ICC51166.2024.10622963>
- [31] —, "Two-dimensional direction-of-arrival estimation using stacked intelligent metasurfaces," *IEEE J. Sel. Areas Commun.*, vol. 42, no. 10, pp. 2786–2802, 2024. [Online]. Available: <https://doi.org/10.1109/JSAC.2024.3414613>
- [32] H. Niu, J. An, A. K. Papazafeiropoulos, L. Gan, S. Chatzinotas, and M. Debbah, "Stacked intelligent metasurfaces for integrated sensing and communications," *IEEE Wirel. Commun. Lett.*, vol. 13, no. 10, pp. 2807–2811, 2024. [Online]. Available: <https://doi.org/10.1109/LWC.2024.3447272>
- [33] S. Li, F. Zhang, T. Mao, R. Na, Z. Wang, and G. K. Karagiannidis, "Transmit beamforming design for isac with stacked intelligent metasurfaces," *IEEE Transactions on Vehicular Technology*, pp. 1–6, 2024.
- [34] C. Pei, K. Huang, L. Jin, X. Xu, Y. Zhou, and Y. Guo, "Stacked intelligent metasurfaces assisted integrated-sensing-and-resistance anti jamming," *IEEE Communications Letters*, pp. 1–1, 2024.
- [35] M. Nerini and B. Clerckx, "Physically consistent modeling of stacked intelligent metasurfaces implemented with beyond diagonal ris," *IEEE Communications Letters*, vol. 28, no. 7, pp. 1693–1697, 2024.
- [36] D. M. Pozar, *Microwave Engineering*, 4th ed. John Wiley & Sons, Inc., 2011.
- [37] X. Lin, A. G. P. M. P. Wang, J. D. O'Brien, and C. G. M. P. M. S. Fortunato, "All-optical machine learning using diffractive deep neural networks," *Science*, vol. 361, no. 6406, pp. 1004–1008, Sep. 2018.